AGU PUBLICATIONS

Journal of Advances in Modeling Earth Systems

RESEARCH ARTICLE
10.1002/2014MS000332

Key Points:
- First time-varying probabilistic ash cloud forecast maps
- High-fidelity probability mapping with moment optimization and high-resolution winds
- Testing of outputs with standard metrics and against multimodel and SKEB

Correspondence to:
M. Bursik,
mib@buffalo.edu

Citation:
Stefanescu, E. R., et al. (2014), Temporal, probabilistic mapping of ash clouds using wind field stochastic variability and uncertain eruption source parameters: Example of the 14 April 2010 Eyjafjallajökull eruption, *J. Adv. Model. Earth Syst.*, *06*, doi:10.1002/2014MS000332.

Received 4 APR 2014
Accepted 12 OCT 2014
Accepted article online 16 OCT 2014

Temporal, probabilistic mapping of ash clouds using wind field stochastic variability and uncertain eruption source parameters: Example of the 14 April 2010 Eyjafjallajökull eruption

E. R. Stefanescu[1], A. K. Patra[1], M. I. Bursik[2], R. Madankan[1], S. Pouget[2], M. Jones[3], P. Singla[1], T. Singh[1], E. B. Pitman[4], M. Pavolonis[5], D. Morton[6], P. Webley[6], and J. Dehn[6]

[1]Department of Mechanical and Aerospace Engineering, University at Buffalo, Buffalo, New York, USA, [2]Department of Geology, University at Buffalo, Buffalo, New York, USA, [3]Center for Computational Research, University at Buffalo, Buffalo, New York, USA, [4]Department of Mathematics, University at Buffalo, Buffalo, New York, USA, [5]NOAA-NESDIS Center for Satellite Applications and Research, Madison, Wisconsin, USA, [6]Geophysical Institute, University of Alaska, Fairbanks, Alaska, USA

Abstract Uncertainty in predictions from a model of volcanic ash transport in the atmosphere arises from uncertainty in both eruption source parameters and the model wind field. In a previous contribution, we analyzed the probability of ash cloud presence using weighted samples of volcanic ash transport and dispersal model runs and a reanalysis wind field to propagate uncertainty in eruption source parameters alone. In this contribution, the probabilistic modeling is extended by using ensemble forecast wind fields as well as uncertain source parameters. The impact on ash transport of variability in wind fields due to unresolved scales of motion as well as model physics uncertainty is also explored. We have therefore generated a weighted, probabilistic forecast of volcanic ash transport with only a priori information, exploring uncertainty in both the wind field and the volcanic source.

1. Introduction

Volcano observatories and volcanic ash advisory centers (VAACs) predict the likely position of ash clouds generated by explosive volcanic eruptions using deterministic mathematical models of advection and dispersion, known as volcanic ash transport and dispersal (VATD) models [*Langmann et al.*, 2012; *Folch*, 2012]. These models require input data on volcanic source conditions as well as the wind field [*Mastin et al.*, 2009]. The resulting maps are often understood to delineate "hard" exclusion zones. In contrast, most meteorological forecasts are issued as maps or reports giving the probability of an event or the occurrence of a phenomenon, like precipitation, in a certain region at a specific time [*Zhang and Krishnamurti*, 1999]. Partly because of this disparity between ash cloud and meteorological forecasting and the desire to produce ash forecast products comparable to the standard, a need has been expressed on numerous occasions for probabilistic ash cloud forecasts [*IVATF*, 2011].

In previous work [*Bursik et al.*, 2012], we analyzed the probability of ash presence using a VATD with a reanalysis wind field, which is only available a posteriori, to propagate uncertainty in volcanic eruption source parameters. In this contribution, we extend the previous work and address the problem of probabilistic volcanic ash transport forecasting by propagation of uncertainties in both the volcanic eruption source parameters and wind fields. To illustrate our methodology, we hindcast the motion of the ash cloud for the eruption of Eyjafjallajökull, Iceland, which had a peak ash emission in the period 14–18 April 2010.

In developing a probabilistic forecast for ash location with time, we thus investigate the effects of aleatoric uncertainty associated with volcanic eruption source parameters and the wind field using suitable ensembles, and epistemic uncertainty associated with the advective equations of motion by investigating outputs of both multiphysics and spectral ensembles. Such an analysis is much needed in complex environments and provides Operational Decision Support using a Dynamic Data-Driven Application System (DDDAS) paradigm [*Patra et al.*, 2013a, 2013b; *Stefanescu et al.*, 2014a, 2014b]. Operational and research flood forecasting

systems around the world are increasingly moving toward using ensembles of NWPs, rather than single deterministic forecasts, to drive their flood forecasting systems. This usually involves using Ensemble Prediction Systems (EPS) as input to a hydrological and/or hydraulic model to produce river discharge predictions, often supported by some kind of Decision Support System. See *Cloke and Pappenberger* [2009] for challenges encountered in flood forecasting, many of which we overcome through our novel approach for ash cloud forecast.

We couple three numerical tools for this analysis. The first is the Weather Research and Forecasting (WRF) model used to forecast wind speed. The second tool is a volcanic eruption column model, bent, employed to incorporate volcano observations and then provide initial conditions for a volcanic ash cloud transport and dispersal (VATD) model. The third tool is a VATD model, PUFF, used to propagate ash parcels in the wind field. PUFF output is a record of ash concentrations in space and time, and we have used this information to estimate the probability of the presence of ash in the atmosphere above the Earth's surface.

Weighted samples were drawn from the random variables in eruption source parameter space of bent using the Conjugate Unscented Transform (CUT) [*Adurthi et al*., 2012; *Madankan et al*., 2013]. CUT is designed to minimize errors in moment computations with a minimal number of samples and obtains accuracies comparable to Monte-Carlo sampling with orders of magnitude fewer samples. The uncertain source parameters are then propagated to outputs suitable to provide initial conditions for a VATD model, PUFFs, which is used to propagate ash parcels in the uncertain wind field.

To characterize the effect of wind on the VATD output, we generate wind field ensembles using the following two methods:

1. Using the Global Ensemble Forecast System (GEFS) as both initial conditions and boundary conditions for WRF to obtain "high-resolution" interpolated wind fields.
2. Changing physics parameters in WRF, which results in different wind fields.

A quantitative comparison of the wind fields resulting from the above two methods against radiosonde data is used to determine which method results in higher variability. High variability means that there is a wider range of outcomes, i.e., a higher probability of capturing the true behavior. In this way we are best able to capture extreme, yet possible, wind fields.

We illustrate the effect of unresolved scales in the NWP using the Stochastic Kinetic Energy Backscatter (SKEB) option in WRF. We observe that using the SKEB option causes greater simulated ash cloud dispersion. This is consistent with the observation of *Berner et al*. [2008] that SKEB increases scatter in vorticity and energy. We explore what happens when forecasts are run for different periods. Thus, we take different forecast start times: 0000 UTC 14 April, or 0000 UTC 16 April, and compare model outputs with satellite data for 0000, 0600, 1200, and 1800 UTC 16 April.

The results of probabilistic forecasts are tested with standard methods against satellite data for the paroxysmal phase of the Eyjafjallajökull eruption of 14–18 April 2010. Probability maps and Receiver Operating Characteristic (ROC) curves are also used to quantify the wind effect in the model output.

2. Background

Measures of eruption intensity and grain size represent some of the major sources for uncertainty in ash transport and dispersion simulations [*Mastin et al*., 2009; *Dacre et al*., 2011; *Bursik et al*., 2012; *Webley et al*., 2012]. Estimates of the magnitude of the uncertainty are also needed. Because of our lack of knowledge of the exact conditions at the volcanic source at the time of an eruption, probability distributions are assigned to the uncertain eruption source parameters, based on samples of past eruptions which have been collected from the historical record, or real-time data that lend some insight into current eruption conditions. We sample the probability density functions using a non-Monte Carlo technique that optimizes moment calculations. In this contribution, simulation ensembles with different input volcanic source parameters are intelligently chosen to predict the average and higher-order moments of the output correctly.

Because of the separate spatial scales and physics, eruption column (volcanic plume) models have generally been developed separately from VATD models. One such eruption column model, bent solves a cross-sectionally averaged system of equations for continuity, momentum, and energy balance. It takes a size

distribution of pyroclasts, then outputs the height distribution of the clasts in the atmosphere [*Bursik*, 2001]. In producing its eruption outputs, bent accounts for atmospheric (wind, temperature, pressure, etc.) conditions as given by atmospheric sounding or NWP data. It has been tested against plume rise height data, and against dispersal data [*Bursik et al*., 2009]. Details of the volcanic source parameters along with assumptions and probability distributions used are presented in *Bursik et al*. [2012] and *Madankan et al*. [2013]. bent simulations output a volume into which particles are placed in the atmosphere around the volcano. These are released into the WRF gridded wind field, and their movement is calculated via the VATD model PUFF.

Given an initial ash-laden volume produced by bent, the PUFF Lagrangian VATD model was used to populate the volume, then propagate ash parcels in ensemble wind fields [*Searcy et al*., 1998]. PUFF simulates the paths of N particles and provides forecasts of the location of a given particle size at a specific time instant. The model takes into account dry particle fallout, as well as dispersion and advection. PUFF does not model wet deposition.

Ensemble modeling, originally developed for weather prediction, is being extended to atmospheric dispersion applications [*Krishnamurti et al*., 2000; *Galmarini et al*., 2004]. Several techniques have been developed over the last decade for the ensemble treatment of atmospheric dispersion model predictions. Among them, two have received most of the attention—the multimodel and the ensemble prediction system (EPS) model [*Potempski et al*., 2008; *Galmarini et al*., 2010]. The multimodel approach relies on model simulations produced by different atmospheric dispersion models using meteorological data from potentially different weather prediction systems. A typical EPS-based ensemble is generated by running a single atmospheric dispersion model with ensemble weather prediction members.

For the atmospheric characterization incorporated into a dispersion model, an EPS-based ensemble is one way to replace a single, deterministic forecast with an estimate of the probability density function of forecast weather states [*Warner*, 2011; *Galmarini et al*., 2004]. There are methods to generate initial condition uncertainty in wind ensembles and produce perturbations that have dynamically consistent structures. At the National Centers for Environmental Prediction (NCEP), *Toth and Kalnay* [1993] introduced the bred-vector (BV) perturbation method to create the Global Ensemble Forecast System (GEFS) wind field forecast.

The model created by propagating both wind field uncertainty via the GEFS ensemble and eruption source parameter uncertainty does not account for improperly characterizing the physics of the atmosphere [*Potempski et al*., 2008]. Using a multiphysics ensemble, one aims to capture the model-related forecast uncertainty by averaging the individual physics members using equal weights.

Due to finite model resolution, the physical processes that span numerous orders of magnitude of spatial scales must be approximated (parameterized). Recently, stochastic parameterization techniques have been applied to capture unresolved or poorly represented scales of motion in such a way that the models have a statistical or spectral behavior that is consistent with observations of the entire atmosphere. The Stochastic Kinetic-Energy Backscatter (SKEB) scheme [*Shutts*, 2005] is one such method to generate a model that is spectrally consistent with the real atmosphere.

3. Methodology

3.1. WRF-bent-PUFF Coupling

To implement the WRF-bent-PUFF coupling, we consider a variable of interest (e.g., ash top height at a specific geolocation). Let this be a random variable, $\mathbf{x}_k$, whose time evolution is given by WRF-bent-PUFF:

$$\dot{\mathbf{x}} = \mathbf{f}(t, \mathbf{x}, \mathbf{\Theta}, \mathcal{W}). \tag{1}$$

In equation (1), $\mathbf{\Theta} = \{\theta_1, \theta_2, \ldots\}$ represents uncertain system parameters such as the vent radius, eruption velocity, mean grain size, and grain size variance and $\mathcal{W}$ is a given wind field from a NWP model.

Weighted samples from the random variables in eruption source parameter space are drawn using the Conjugate Unscented Transform (CUT) [*Adurthi et al*., 2012; *Madankan et al*., 2013] and are then combined in a tensor-product fashion with each wind ensemble member. The main idea of the CUT approach is to select specific structures for symmetric points, rather than taking a tensor product of 1-D points as in the Gauss quadrature scheme. As a result, the quadrature points still exactly integrate polynomials of total degree

$2N-1$ in n-dimensional space, while the number of points is much less than N^n. Here N represents the number of quadrature points needed to solve a one-dimensional integral (according to the Gaussian quadrature scheme).

The probability of ash top height is given by

$$P(h)=\int_{\Omega} P(h|W)p(W)dW \approx \frac{1}{N_W}\sum_{i=1}^{N_W} P(h|W_i) \tag{2}$$

while the expected value of ash top height is

$$\begin{aligned} E[h]&=\int_{\Omega} hP(h)dh=\int_{\Omega_W} h(\theta,W)\left(\int_{\Omega_S} P(h|W)p(W)dW\right)dh \\ &=\int_{\Omega_W}\int_{\Omega_S} h(\theta,W)P(h|W)p(W)dW\,dh \\ &=\sum_{i=1}^{N_W} w_i \sum_{q=1}^{N_{CUT}} w_q h(\theta_q,W_i), \end{aligned} \tag{3}$$

where w_i are the weights associated with the wind ensemble, while w_q are those for the eruption source parameters obtained from using a generalized polynomial chaos (gPC) expansion [*Bursik et al*., 2012]. Ω_W and Ω_S are the wind field parameter space and eruption source term parameter space, respectively.

3.2. GEFS Ensemble Forecast

Major factors that influence the accuracy of NWP models are the resolution of the grid, uncertainty in the initial observations, and the use of different parameterization schemes. For wind fields, ensemble methods are considered to be an effective way to estimate the probability density function [*Mann*, 1998] of future states of the atmosphere by addressing uncertainties present in initial conditions and in model approximations. Ensemble forecasting provides human forecasters with a range of possible solutions, whose average is generally more accurate than the single deterministic forecast [*Kalnay*, 2003], and whose spread provides a quantitative basis for probabilistic forecasting. In terms of dispersion modeling, ensemble forecasting becomes more important when the dispersion simulations are forecasts for which there are sparse satellite data for validation, and when the model results are used for decision support or regulatory purposes [*Galmarini et al*., 2010]. To construct the ensemble ash forecast then, output statistics of the volcanic ash location and three-dimensional ash concentrations (the height at the top of an ash cloud-ash top height can be extracted from these) are computed by properly summing the weighted values of the output parameters of interest.

Iceland's Eyjafjallajökull volcano first erupted on 14 April 2010. Volcanic ash was emitted up to a height of 11 km [*Langmann et al*., 2012] and was advected to the east by the local weather system. For these eruptive events of April 2010, we use the 21 member NCEP "high resolution" GEFS forecasts produced four times daily [*Toth and Kalnay*, 1993] on a 1° latitude by 1° longitude grid. Two GEFS forecasts are used—one with a start time of 0000 UTC 14 April and the other 0000 UTC 16 April; output is retrieved for both cases up to 0000 UTC 18 April. By using these forecasts with different start times, we are able to construct and compare forecasts with 48 h and 0 h lead times, respectively. In the first case, outputs are at forecast hours 48, 54, 60, and 66; in the latter case, the outputs are at forecast hours 0, 6, 12, and 18. For the period before this from the start of the eruption at approximately 0000 UTC 14 April, we use NCEP/NCAR Reanalysis data as a deterministic realization of the wind fields as input to the VATD model. To generate high-resolution forecast wind fields from GEFS, the Weather Research and Forecasting-Advanced Research WRF (WRF-ARW) numerical weather prediction system [*Skamarock et al*., 2005; *UCAR*, 2012] is used to interpolate GEFS outputs. The main physical options used in WRF include Kessler microphysics, Mellor-Yamada-Janjic planetary boundary layer (PBL) scheme [*Noh et al*., 2003], and the Noah land surface model [*Chen and Dudhia*, 2001]. For each GEFS member forecast, a continuous WRF run/integration with a single GEFS initialization is done, resulting in outputs every 3 h at 74 pressure levels. The model domain is organized around the location of the

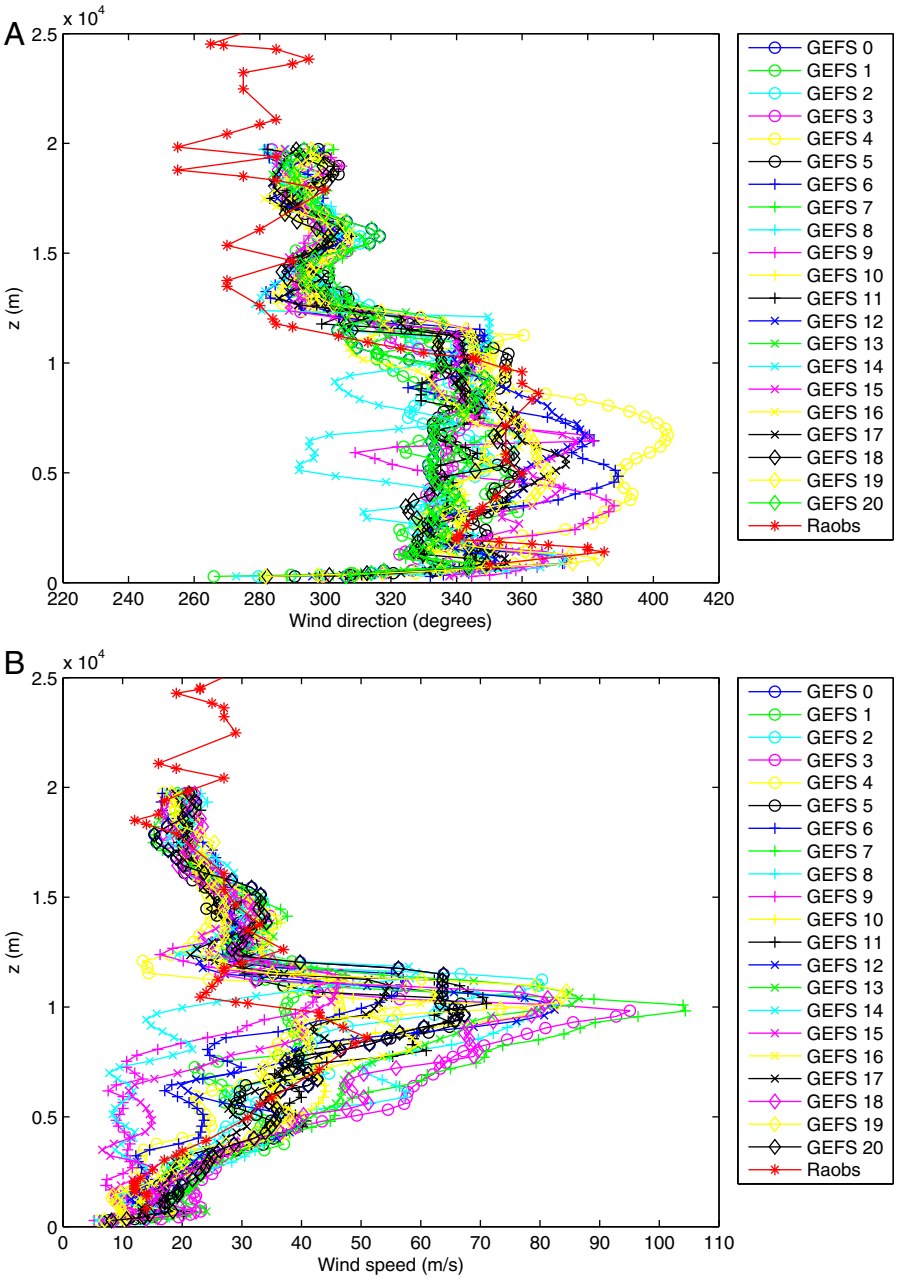

Figure 1. Comparison of wind direction (degrees) and wind speed (m/s) from radiosondes with those from GEFS Praha-Libus station–72 h forecast.

Eyjafjallajökull vent (63.63°N and 19.63°S) with dimensions of 230 × 230 horizontal grid points at a spacing of 27 km, with 29 pressure levels (1000–100 hPa, excluding the surface) and comprises most of Europe.

3.3. Multiphysics Ensemble Forecast

To understand the effects of the paucity of information (epistemic uncertainty) about which physics approaches to use in WRF, we test WRF by comparing results from ensemble runs having different combination of physics options (Kessler microphysics = 1, 4, and 6; PBL = 2, 4, and 5; Noah land surface model = 1 and 4). Specifically, we test if different WRF physics options are important in light of the uncertainty generated by GEFS by comparing multiphysics and GEFS outputs with radiosonde data. We decided, a priori, that the approach (multiphysics or GEFS) yielding the greatest variance in the wind field prediction would be

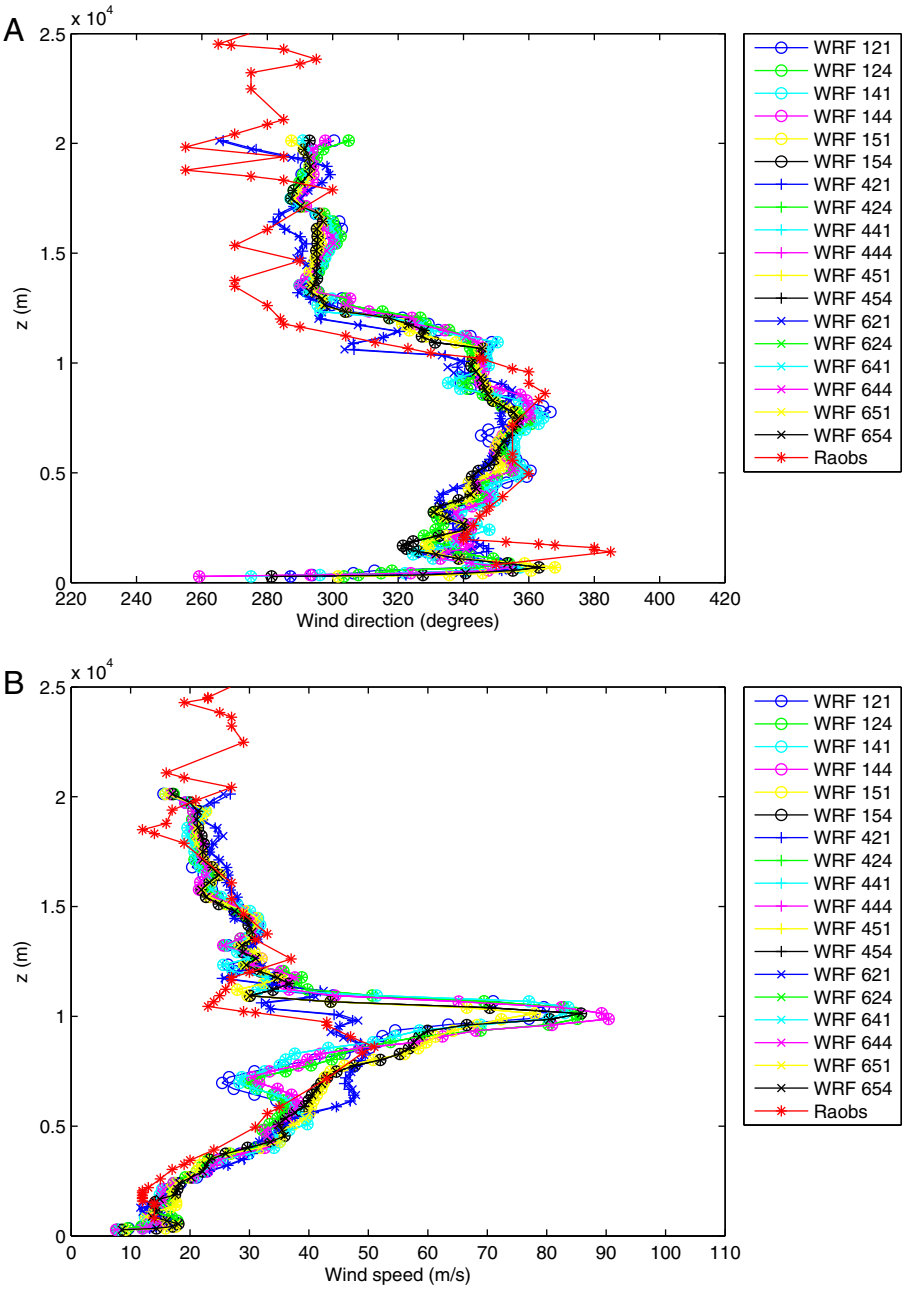

Figure 2. Comparison of wind direction (degrees) and wind speed (m/s) from radiosondes with those from WRF multiphysics output at Praha station–72 h forecast where the first digit in the WRF XXX represents the Microphysics value, the second digit PBL, and third digit K as in *UCAR* [2012].

the one to be used in the simulations, as it would presumably yield the greatest dispersion of ash cloud probability.

We perform a simple test of the potential effects of the multiphysics ensemble. The test consists of checking wind direction and amplitude forecasts from the two ensemble techniques with radiosonde data [*UWYO*, 2012] at Praha-Libus, Czech Republic, at 50.00°N and 14.45°E (Figure 1). We compare with radiosonde data since wind velocity is no doubt the most important control on ash cloud motion. We find that multiphysics ensembles sometimes generate dramatically less variability in forecast wind fields than do GEFS initial-condition ensembles (Figure 2). This result suggests that, in the present case, the GEFS ensemble is a better choice to most fully capture wind field variability to be used in calculating probabilistic ash hazards maps.

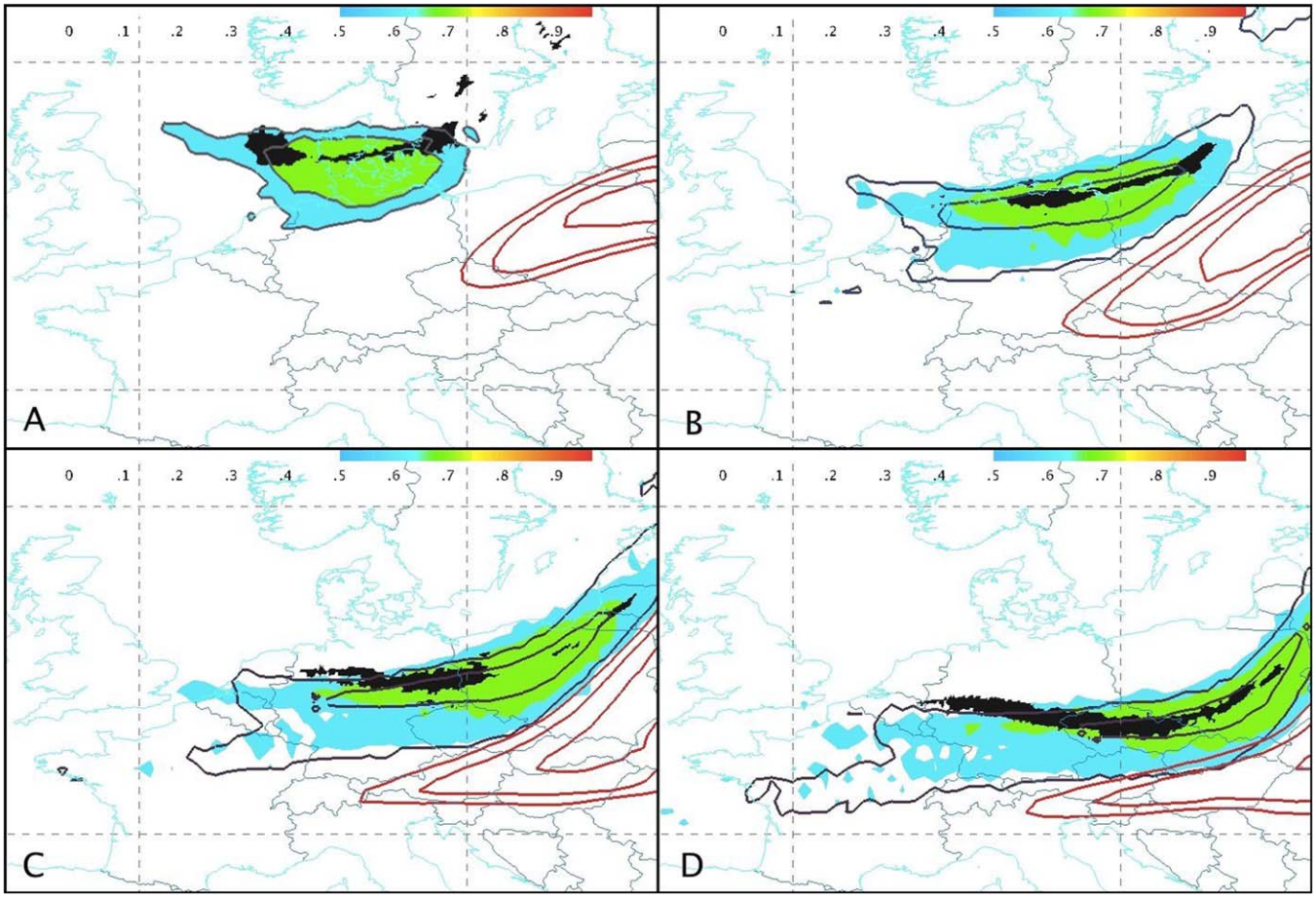

Figure 3. Average probability of having airborne ash when accounting for source parameter uncertainty only (color fill); or both uncertain source parameters and wind field variability—forecast starting 0000 UTC 16 April (black probability contour); source parameters and wind field variability—forecast starting 0000 UTC 14 April (red probability contour), and corresponding satellite image (black fill). Blue fill—probability = 0.5; green fill—probability = 0.7. Outer black contour—probability = 0.5; inner black contour—probability = 0.7. Outer red contour—probability = 0.5; middle red contour—probability = 0.7; inner red contour—probability = 0.9. The 0.9 contour is visible, neither in the color fill nor in the black contour maps, as it is smaller than single pixels in these products. (a) 0000 UTC 16 April, (b) 0600 UTC 16 April, (c) 1200 UTC 16 April, and (d) 1800 UTC 16 April.

3.4. Stochastic Kinetic-Energy Backscatter (SKEB)

Forward time integration is performed using numerical models designed to simulate different physical processes in the atmosphere. These processes are active at scales smaller than the grid size used in the numerical integration and thus remain unresolved and can only be approximated [*Buizza and Palmer*, 1995; *Shutts*, 2005; *Berner et al*., 2008]. This misrepresentation of unresolved subgrid-scale processes is deemed to be model error and may be addressed by introducing a stochastic element into atmospheric models by randomly perturbing the increments or tendencies from parameterization schemes [*Buizza et al*., 1999; *Palmer et al*., 2009]. Other approaches seek to formulate the parameterization schemes in a stochastic way [*Palmer and Williams*, 2008; *Plant and Craig*, 2008]. Here, we explore the potential effects of the unresolved subgrid scale processes by using a Stochastic Kinetic Energy Backscatter (SKEB) algorithm [*Shutts*, 2005, 2008], which is a simplified version of the algorithm of *Berner et al*. [2009]. The SKEB scheme is based on the notion that the turbulent dissipation rate is a function of the difference between upscale and downscale spectral kinetic energy transfer [*Shutts*, 2005]. The scheme implemented here assumes a spatially and temporally constant dissipation rate.

The stochastic perturbation fields for wind and temperature are controlled by the kinetic and potential energy injected into the flow. The injected energy is expressed as a backscattered dissipation rate for the streamfunction and temperature, respectively. To investigate the potential variability introduced by our lack of properly characterizing the spectral characteristics of the atmospheric motion with SKEB, WRF simulations are performed for the same time period, and same initial conditions and physics options, as described

above for the Eyjafjallajökull eruption with SKEB option ON or OFF. We then visualize the potential variability introduced by SKEB by comparing ash cloud positions and shapes.

Remark: While ensembles are often used to characterize the potential spread in outcomes based on input variability, our objective here is different. The source parameter ensemble is chosen such that weighted combinations of ensemble model evaluation outcomes (e.g., ash top height) provide estimates of expectation, variance, and probabilities of occurrence of the outcome as would be obtained by statistics from a much larger random sampling. The tensor product of the GEFS ensemble for winds with this model ensemble produces a product that reflects the variability in both the source parameters and wind fields. Additionally, we also illustrate the effect of unresolved scales using the SKEB as outlined here.

3.5. Construction of Probabilistic Maps

To produce the probabilistic forecast, we thus use each GEFS ensemble member as WRF input, keeping physics and dynamics options the same for all runs. The ensemble wind field is then constructed from the high-resolution WRF models, each of which uses a separate GEFS ensemble member for boundary conditions. Samples from the random variables of eruption velocity, vent radius, mean grain size, and grain size standard deviation in eruption source parameter space are drawn using the CUT method.

Following runs of bent at the CUT sample points, each bent output is propagated through PUFF, for each WRF ensemble member. The outputs from PUFF are then combined in a tensor-product fashion by applying the appropriate weight to each deterministic WRF-bent-PUFF run. Use of the CUT method results in 161 quadrature points (for four dimensions of uncertain input eruption source parameters), combined with a 21-member wind ensemble, leading to 3381 simulation runs. The result is a map of the probability of having airborne ash at a point, which is compared with satellite images (Figure 3). The Spinning Enhanced Visible and Infrared Imager (SEVIRI) on board the Meteosat Second Generation (MSG) satellite played a critical role in tracking the Eyjafjallajökull ash clouds with high temporal resolution. While multispectral SEVIRI imagery is an effective tool for manually tracking volcanic ash clouds, SEVIRI can also be used to retrieve the ash cloud top height, mass loading, and effective particle radius, which are important for nowcasting and forecasting ash cloud locations. At present, examination of satellite (SEVIRI) data provides the best quantitative method for detecting and analyzing ash clouds.

4. Results and Discussion

In this contribution, we forecast ash cloud movement by treating the wind as a random variable along with the volcanic input parameters of vent radius, eruption velocity, mean grain size, and grain size variance. To discuss uncertainty and its effects on models, we distinguish between parametric uncertainty and wind field forcing uncertainty. Methodologically, these two kinds of uncertainty are accounted for differently. In a deterministic setting, ash top height at a given time and location is based on integration of advected PUFF particles. In developing a probabilistic forecast for the ash location, we treat the model outputs at a given location and time as random variables, and the appropriate output from each "run" of the WRF-bent-PUFF simulation is a sample from that random variable.

The procedure used to calculate the probability of the presence of ash in the atmosphere was introduced in *Bursik et al*. [2012] and is extended here to account for the new uncertainty in the wind field. The effect of the uncertainty in the wind field on the forecast has been evaluated by standard meteorological measures of error and goodness-of-fit. In the case of the combined WRF-bent-PUFF runs, we have evaluated the statistical properties of the ensemble forecasts using two measures that can be applied in cases where a probabilistic meteorological forecast is being tested against binary observations, in our case the presence or absence of an ash cloud in SEVIRI data [see *Bursik et al*., 2012], or in deterministic wind field reanalysis runs. Because data from any one instrument do not necessarily yield the position of all airborne ash, and because we seek to understand the specific effects of the wind field ensemble, the model outputs must be understood relative to one another as well as in an absolute sense. Nevertheless, there is reason to believe that SEVIRI provides the best estimate of airborne ash from any single instrument available for the eruption under consideration [*Bursik et al*., 2012].

Qualitative snapshots comparing the performance of models with and without wind field uncertainty are shown in Figure 3. It can be observed that probability maps for both reanalysis and GEFS models rather

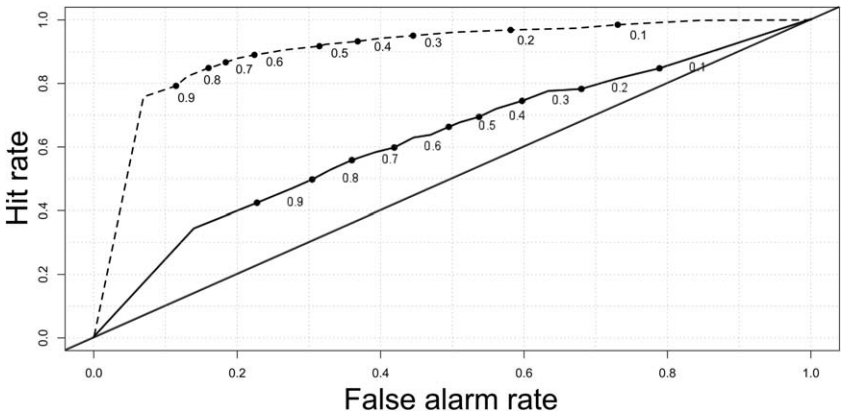

Figure 4. Receiver Operating Characteristic (ROC) curve for maximum ash with concentration exceeding 10^{-10} mg/m^3, for source parameters and wind field variability used as model, and source parameters only used as basis of comparison. Dashed curve, forecast starts after 0000 UTC 16 April; solid curve, forecast starts after 0000 UTC 14 April. Numbers next to curves are probability thresholds to forecast presence of ash. The hit rate is defined as the number of times the event was both forecast (uncertain source parameters and ensemble wind fields both used) and observed (source parameters only used) to occur. The false alarm rate records the number of cells in which ash was forecast, but there was no ash present.

thoroughly cover the region where volcanic ash exists according to satellite imagery, given a 0 h wind field forecast. The match between model and data is much worse when using a 48 h wind field forecast, as would be expected.

We can evaluate the comparisons between model and data in a quantitative fashion by using the Brier Score. The Brier Score in the present context is the mean squared difference between the probability of ash assigned by the forecast to a particular position, and the absence (=0) or presence (=1) of ash in the SEVIRI image. The Brier Score calculated from the use of reanalysis data is equal to 0.3225, while for the GEFS 0 h forecast data, it is 0.2048. Since Brier score is a measure of error, smaller values are better. Thus, even though use of the GEFS ensemble introduces more variability, the error in the forecast actually decreases, as the ensemble produces a 0 h forecast that better matches SEVIRI data than does the use of reanalysis data. This is confirmed by the Figure of Merit in Space, which is 0.148 when reanalysis data are used and 0.165 when the GEFS ensemble is used. This must mean, enigmatically and perhaps serendipitously, that the GEFS ensemble forecast better represents the true wind field than does the reanalysis. We believe that this result must arise from the fact that within a single data assimilation cycle, the higher spatial resolution WRF model used with GEFS provides a better estimate of the wind field than does reanalysis data.

PUFF output is a record of ash concentrations in space and time, and we have used this information to extract the height at the top of an ash cloud (defined as the maximum height at which ash concentration exceeds 10^{-10}mg/m^3). We thus use the Receiver Operating Characteristic (ROC) curve to further explore the difference between the use of GEFS forecast data as opposed to reanalysis in the wind fields. The ROC curve is usually used to provide information on the hit and false alarm rates that are obtained by probabilistic model output compared to binary "present/absent" data. In our case, we use the ROC curve to compare output at April 16 0600 UTC using the GEFS ensemble and eruption source parameter uncertainty as a continuous probability (the "model"), with output using reanalysis data and eruption source parameter uncertainty reduced to a binary presence or absence of ash (the "data"). A cell is defined to contain ash if the *maximum ash concentration exceeding* 10^{-10}mg/m^3 > 0. Hit and false alarm rates are plotted at different probability thresholds. These express whether the model is consistent with the data ("hit"), or whether the model predicted ash where there was no ash in the data ("false alarm") (Figure 4). The area under the ROC curve is often used as a single summary measure. A larger area is better (a perfect forecast has area = 1). When we compare the area under the curve for the two forecasts at 0 h and at 48 h, for the 0 h forecast we get a better approximation of the reanalysis footprint (area = 0.903), than we do for the 48 h forecast (area- = 0.622). The ROC score indicates that within a single 24 h model cycle, the forecast position of the ash cloud remains close to the reanalysis position, whereas they diverge considerably after 2 days. This particular divergence of forecast "model" from reanalysis "data" is the result of the lack of fidelity in the forecast

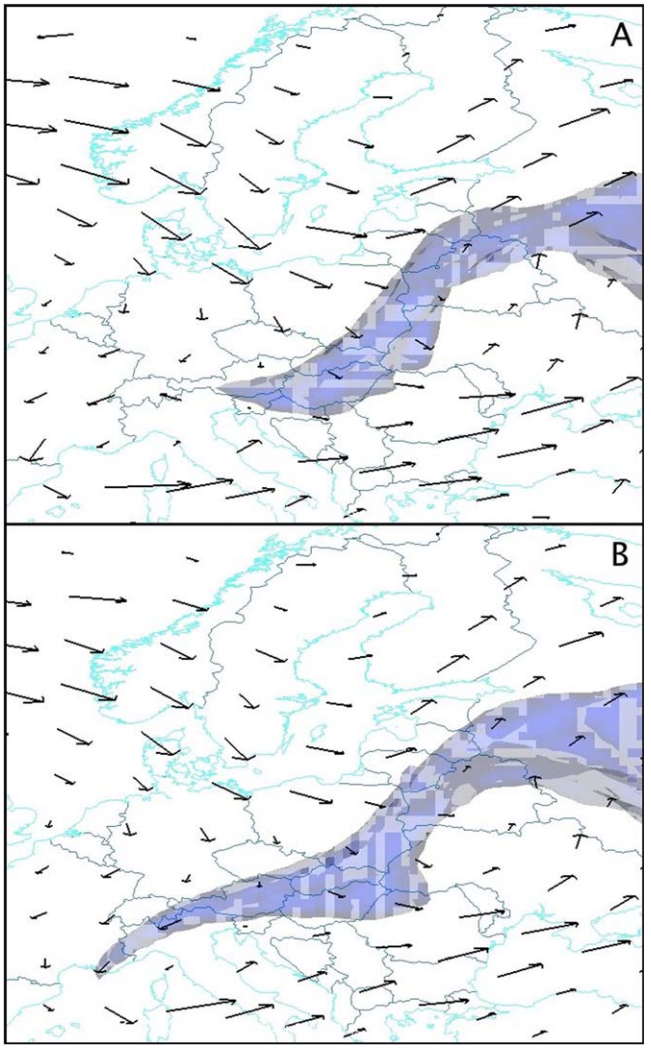

Figure 5. The 0000 UTC 16 April forecast starting 0600 UTC 14 April (a) without SKEB compared to the same forecast (b) with SKEB. Note the slightly greater extent of the ash cloud in Figure 5b.

wind field over multiple data assimilation cycles, since there is no difference in eruption source parameters. ROC curves at different forecast time display similar behavior.

We have already touched upon the effects of the multiphysics approach in our evaluation of the forecast radiosondes (Figure 2). The multiphysics approach seems to introduce less variability than GEFS into the wind field. We therefore did not pursue any PUFF runs with the multiphysics ensemble. However, to explore the potential effects of greater uncertainty in ash cloud position resulting from unresolved, short wavelength scales of wind field motion (related to "underdispersiveness" in NWP ensembles [*Berner et al.*, 2009]), WRF simulations are performed using the SKEB scheme, with realizations of PUFF being run with SKEB on or off and the outputs compared (Figure 5). The results suggest that SKEB indeed causes greater ash cloud dispersion, possibly by increasing scatter in vorticity and energy at length scales of hundreds of km. The result on ash dispersion as shown by comparing PUFF runs is primarily to increase the stretching mode of the ash cloud more than the bending and diffusion modes as defined by *Bursik* [1998]. Although application of SKEB does therefore result in an ensemble ash cloud of greater extent, the ensemble still contains insufficient variability to encompass the observed ash cloud given a 48 h forecast. This may be because SKEB does not introduce sufficient variability at the synoptic scale.

5. Conclusions

For the first time, ash transport simulation results are presented as time-varying, probabilistic forecast maps of ash clouds that reflect the effects of both eruption source parametric uncertainty and wind field stochastic variability. We do this by using the conjugate unscented transform (CUT) algorithm to create a parsimonious sample of the input eruption source parameter space that optimizes moment calculation. This is combined in a tensor product with high-resolution Weather Research and Forecasting (WRF) wind fields generated from the GEFS ensemble prediction system (EPS) to create a probabilistic map of the output space of ash presence overhead with a sample size of only ~3000 members. A Monte-Carlo sample of comparable fidelity would probably consist of 10^5 to 10^6 members, and be computationally impractical. We tested the reliability of the forecasts qualitatively, as well as quantitatively using standard meteorology metrics. The results in this present case suggest that ensemble or probabilistic forecasting of ash cloud motion can yield reasonable probability envelopes given standard 0–24 h forecasts, without using source-

parameter inversion, Bayesian updating or Kalman filtering. These methodologies have been shown elsewhere, however, to improve the details of the local footprint of the forecast model relative to later satellite data acquisitions [*Stohl et al*., 2011; *Denlinger et al*., 2012; *Madankan et al*., 2012, 2013].

To study the limitations of the use of the GEFS-EPS for the wind fields, we create outputs using multiphysics wind fields, as well as the Spectral Kinetic Energy Backscatter (SKEB) technique (both within WRF). The resulting maps explore the potential for greater spread in the ash cloud probability density function that would enable the probabilistic forecast to better encompass observed ash cloud occurrences at greater forecast times. A qualitative evaluation of the outputs suggests that neither multiphysics nor SKEB is capable of injecting sufficient uncertainty at short-wavelengths to fully encompass ash cloud positions in forecasts at 48 h.

In the future, we seek to integrate improved estimates of mass eruption rate and mass loading into the eruption source parameter calculations [*Pouget et al*., 2013], as well as source parameter inversion or Bayesian updating, as appropriate [*Madankan et al*., 2013]. The first would perhaps make possible reasonable estimation of mass loading and concentration as well as ash cloud position, and the latter better estimation of the short-wavelength footprint at greater forecast time.

Acknowledgments

We thank Stefano Galmarini and Judith Berner for useful discussions regarding this work. We thank an anonymous Associate Editor of JAMES for useful feedback on a previous submission. The work reported herein was supported by AFOSR contract number FA9550-11-1-0336, and by NSF CMMI-1131074. All results and opinions expressed in this article are those of the authors and do not reflect opinions of NSF or AFOSR. The authors acknowledge the Atmospheric Sounding portal of the University of Wyoming (http://weather.uwyo.edu/upperair/sounding.html) for providing the radiosonde data. Satellite data used in the analyses and computational outputs are available from the authors.

References

Adurthi, N., P. Singla, T. Singh (2012), The Conjugate Unscented Transform–An approach to evaluate multi-dimensional expectation integrals, *American Control Conference (ACC)*, pp. 5556–5561, IEEE, Montreal, QC.

Berner, J., F. Doblas-Reyes, T. Palmer, G. Shutts, and A. Weisheimer (2008), Impact of a quasi-stochastic cellular automaton backscatter scheme on the systematic error and seasonal prediction skill of a global climate model, *Philos. Trans. R. Soc. A*, *366*(1875), 2559–2577.

Berner, J., G. Shutts, M. Leutbecher, and T. Palmer (2009), A spectral stochastic kinetic energy backscatter scheme and its impact on flow-dependent predictability in the ECMWF ensemble prediction system, *J. Atmos. Sci.*, *66*(3), 603–626.

Buizza, R., and T. Palmer (1995), The singular-vector structure of the atmospheric global circulation, *J. Atmos. Sci.*, *52*(9), 1434–1456.

Buizza, R., M. Milleer, and T. Palmer (1999), Stochastic representation of model uncertainties in the ECMWF ensemble prediction system, *Q. J. R. Meteorol. Soc.*, *125*(560), 2887–2908.

Bursik, M. (2001), Effect of wind on the rise height of volcanic plumes, *Geophys. Res. Lett.*, *18*, 3621–3624.

Bursik, M. (1998), Tephra dispersal, in The Physics of Explosive Volcanic Eruptions, *Geol. Soc. London Spec. Publ.*, *145*, 115–144.

Bursik, M., S. Kobs, A. Burns, O. Braitseva, L. Bazanova, I. Melekestsev, A. Kurbatov, and D. Pieri (2009), Volcanic plumes and the wind: Jetstream interaction examples and implications for air traffic, *J. Volcanol. Geotherm. Res.*, *186*, 60–67.

Bursik, M., et al. (2012), Estimation and propagation of volcanic source parameter uncertainty in an ash transport and dispersal model: Application to the Eyjafjallajokull plume of 14–16 April 2010, *Bull. Volcanol.*, *74*, 2321–2338.

Chen, F., and J. Dudhia (2001), Coupling and advanced land surface-hydrology model with the Penn State-NCAR MM5 modeling system. Part I: Model implementation and sensitivity, *Mon. Weather Rev.*, *129*, 569–585.

Cloke, H. L., and F. Pappenberger (2009), Ensemble flood forecasting: A review, *J. Hydrol.*, *375*(34), 613–626, doi:10.1016/j.jhydrol.2009.06.005.

Dacre, H., A. Grant, R. Hogan, S. Belcher, D. Thomson, B. Devenish, F. Marenco, M. Hort, J. M. Haywood, and A. Ansmann (2011), Evaluating the structure and magnitude of the ash plume during the initial phase of the 2010 Eyjafjallajökull eruption using lidar observations and NAME simulations, *J. Geophys. Res.*, *116*, D00U03, doi:10.1029/2011JD015608.

Denlinger, R. P., M. Pavolonis, and J. Sieglaff (2012), A robust method to forecast volcanic ash clouds, *J. Geophys. Res.*, *117*, D13208, doi:10.1029/2012JD017732.

Folch, A. (2012), A review of tephra transport and dispersal models: Evolution, current status, and future perspectives, *J. Volcanol. Geotherm. Res.*, *235–236*, 5556–5561.

Galmarini, S., R. Bianconi, W. Klug, T. Mikkelsen, R. Addis, S. Andronopoulos, P. Astrup, A. Baklanov, J. Bartniki, and J. Bartzis (2004), Ensemble dispersion forecasting - Part I: Concept, approach and indicators, *Atmos. Environ.*, *38*(28), 4607–4617.

Galmarini, S., F. Bonnardot, A. Jones, S. Potempski, L. Robertson, and M. Martet (2010), Multi-model vs. EPS-based ensemble atmospheric dispersion simulations: A quantitative assessment on the ETEX-1 tracer experiment case, *Atmos. Environ.*, *44*(29), 3558–3567.

IVATF (2011), International volcanic ash task force (IVATF)—Second Meeting. [Available at http://www.icao.int/safety/meteorology/ivatf/Meeting%20MetaData/IVATF.2.WP.012.2.en.pdf.]

Kalnay, E. (2003), *Atmospheric Modeling, Data Assimilation, and Predictability*, Cambridge Univ. Press, Cambridge, U. K.

Krishnamurti, T. N., C. Kishtawal, Z. Zhang, T. LaRow, D. Bachiochi, E. Williford, S. Gadgil, and S. Surendran (2000), Multimodel ensemble forecasts for weather and seasonal climate, *J. Clim.*, *13*(23), 4196–4216.

Langmann, B., A. Folch, M. Hensch, and V. Matthias (2012), Volcanic ash over Europe during the eruption of Eyjafjallajökull on Iceland, April–May 2010, *Atmos. Environ.*, *48*, 1–8.

Madankan, R., P. Singla, A. Patra, M. Bursik, J. Dehn, M. Jones, M. Pavolonis, B. Pitman, T. Singh, and P. Webley (2012), Polynomial chaos quadrature-based minimum variance approach for source parameters estimation, *Proc. Comput. Sci.*, *9*, 1129–1138.

Madankan, R., S. Pouget, P. Singla, M. Bursik, J. Dehn, M. Jones, A. Patra, M. Pavolonis, E. Pitman, and T. Singh (2013), Computation of probabilistic hazard maps and source parameter estimation for volcanic ash transport and dispersion, *J. Comput. Phys.*, *271*, 39–59.

Mann, J. (1998), Wind field simulation, *Probab. Eng. Mech.*, *13*(4), 269–282.

Mastin, L., M. Guffanti, R. Servranckx, P. Webley, S. Barsotti, K. Dean, A. Durant, J. Ewert, A. Neri, and W. Rose (2009), A multidisciplinary effort to assign realistic source parameters to models of volcanic ash-cloud transport and dispersion during eruptions, *J. Volcanol. Geotherm. Res.*, *186*(1), 10–21.

Noh, Y., W. Cheon, S.-Y. Hong, and S. Raash (2003), Improvement of the K-profile model for the planetary boundary layer based on large eddy simulation data, *Boundary Layer Meteorol.*, *107*, 401–427.

Palmer, T., and P. D. Williams (2008), Introduction. stochastic physics and climate modelling, *Philos. Trans. R. Soc. A*, *366*(1875), 2419–2425.

Palmer, T., R. Buizza, F. Doblas-Reyes, T. Jung, M. Leutbecher, G. Shutts, M. Steinheimer, and A. Weisheimer (2009), *Stochastic Parameterization and Model Uncertainty*, Eur. Cent. for Medium-Range Weather Forecasts, 42 pp., Technical Memorandum 598, Reading, England, U. K.

Patra, A., et al. (2013a), Challenges in developing DDDAS based methodology for volcanic ash hazard analysis—Effect of numerical weather prediction variability and parameter estimation, *Proc. Comput. Sci.*, *18*, 1871–1880.

Patra, A. K., et al. (2013b), A framework for uncertainty quantification for volcanic ash dispersion phenomena, Abstract V23B-2809 presented at AGU Fall Meeting, AGU, San Francisco.

Plant, R., and G. C. Craig (2008), A stochastic parameterization for deep convection based on equilibrium statistics, *J. Atmos. Sci.*, *65*(1), 87–105.

Potempski, S., S. Galmarini, R. Addis, P. Astrup, S. Bader, R. Bellasio, R. Bianconi, F. Bonnardot, R. Buckley, and R. D'Amours (2008), Multi-model ensemble analysis of the ETEX-2 experiment, *Atmos. Environ.*, *42*(31), 7250–7265.

Pouget, S., M. Bursik, P. Webley, J. Dehn, and M. Pavolonis (2013), Estimation of eruption source parameters from umbrella cloud or downwind plume growth rate, *J. Volcanol. Geotherm. Res.*, *258*, 100–112.

Searcy, C., K. Dean, and B. Stringer (1998), PUFF: A high-resolution volcanic ash tracking model, *J. Volcanol. Geotherm. Res.*, *80*, 1–16.

Shutts, G. (2005), A kinetic energy backscatter algorithm for use in ensemble prediction systems, *Q. J. R. Meteorol. Soc.*, *131*(612), 3079–3102.

Shutts, G. (2008), The forcing of large-scale waves in an explicit simulation of deep tropical convection, *Dyn. Atmos. Oceans*, *45*(1), 1–25.

Skamarock, W., J. Klemp, J. Dudhia, D. Gill, D. Barker, W. Wang, and J. Powers (2005), A description of the advanced research WRF Version 2, *Tech. Note NCAR/TN-468+STR*, Natl. Cent. for Atmos. Res., Boulder, Colo.

Stefanescu, E. R., et al. (2014a), Fast construction of surrogates for UQ central to DDDAS—Application to volcanic ash transport, *Proc. Comput. Sci.*, *29*, 1227–1235.

Stefanescu, E. R., A. Patra, M. Bursik, E. Pitman, T. Singh, and P. Singla (2014b), Multiscale method for hazard map construction, to appear in *Proceedings of The Dynamic Data-driven Environmental Systems Science Conference*.

Stohl, A., A. Prata, S. Eckhardt, L. Clarisse, A. Durant, S. Henne, N. Kristiansen, A. Minikin, U. Schumann, and P. Seibert (2011), Determination of time-and height-resolved volcanic ash emissions and their use for quantitative ash dispersion modeling: The 2010 Eyjafjallajökull eruption, *Atmos. Chem. Phys.*, *11*(9), 4333–4351.

Toth, Z., and E. Kalnay (1993), Ensemble forecasting at NMC: The generation of perturbations, *Bull. Am. Meteorol. Soc.*, *74*, 2317–2330.

UCAR (2012), Users Guide for the Advanced Research WRF (ARW) Modeling System Version 3.4. [Available at http://www.mmm.ucar.edu/wrf/users/docs/user_guide_V3/contents.html.]

UWYO (2012), Lerwick and Praha Observations. [Available at http://weather.uwyo.edu/upperair/sounding.html.]

Warner, T. T. (2011), *Numerical Weather and Climate Prediction*, vol. 526, Cambridge Univ. Press, Cambridge, U. K.

Webley, P., T. Steensen, M. Stuefer, G. Grell, S. Freitas, and M. Pavolonis (2012), Analyzing the Eyjafjallajökull 2010 eruption using satellite remote sensing, lidar and WRF-Chem dispersion and tracking model, *J. Geophys. Res.*, *117*, D00U26, doi:10.1029/2011JD016817.

Zhang, Z., and T. Krishnamurti (1999), A perturbation method for hurricane ensemble predictions, *Mon. Weather Rev.*, *127*(4), 447–469.